Food Hydrocolloids 158 (2025) 110553

Contents lists available at ScienceDirect

Food Hydrocolloids

journal homepage: www.elsevier.com/locate/foodhyd

Emulsification capacity of pectin extracts from persimmon waste: Effect of structural characteristics and pectin-polyphenol interactions

Anna Molet-Rodríguez [a,b], Daniel A. Méndez [c], Amparo López-Rubio [c], María José Fabra [c], Marta Martínez-Sanz [d], Laura Salvia-Trujillo [a,b], Olga Martín-Belloso [a,b,*]

[a] Department of Food Technology, University of Lleida, Av. Alcalde Rovira Roure 191, 25198, Lleida, Spain
[b] Agrotecnio CERCA Center, Av. Alcalde Rovira Roure 191, 25198, Lleida, Spain
[c] Food Safety and Preservation Department, Institute of Agrochemistry and Food Technology (IATA), CSIC, Valencia, Spain
[d] Instituto de Investigación en Ciencias de la Alimentación, CIAL (CSIC-UAM, CEI UAM + CSIC), Nicolás Cabrera, 9, 28049, Madrid, Spain

ARTICLE INFO

Keywords:
Persimmon
Pectin
Polyphenols
Molecular structure
Emulsification
Colloidal stability

ABSTRACT

Polyphenol-rich pectin extracts obtained from persimmon waste might have great potential due to their emulsification capacity. Their emulsion stabilizing properties may be influenced by pectin molecular structure and pectin-polyphenol interactions which in turn can be determined by the extraction conditions. Hence, this work aimed to study the influence of the molecular structure characteristics and their respective pectin-polyphenol interactions of three polyphenol-rich persimmon pectin extracts obtained by three different extraction conditions. Low, medium and high severity extraction conditions resulted in covalent phenolics-extract (CP-E), non-covalent phenolics-extract (NCP-E) and free phenolics-extract (FP-E), respectively. The electrical charge of pectin was strongly dependent on the pH, becoming more negative at increasing pH due to carboxyl group dissociation. CP-E and NCP-E in solution had more expanded conformations than FP-E, with greater intermolecular distances and hydrodynamic diameters ranging from 1089 to 1791 nm for CP-E and NCP-E, whereas from 529 to 782 nm for FP-E. Their interfacial layer thickness was thicker at pH 3 than at pH 7, probably due to multilayer organization as a result of less repulsion between pectin chains. All pectin extracts were able to decrease the interfacial tension of an oil droplet from 35 to at least 25 mN/m, with FP-E at pH 3 being the most efficient (13.89 ± 1.07 mN/m). Even so, submicron O/W emulsions with negative ζ-potential values could be formed with all pectin extracts. However, CP-E rendered O/W emulsions with higher colloidal stability than FP-E or NCP-E, which showed aggregation and creaming. These findings provide novel insights to re-valorize pectin from persimmon waste.

1. Introduction

O/W emulsions, consisting of lipid droplets (from 100 nm to 10 μm) dispersed into a continuous aqueous phase, have great potential as delivery systems of lipophilic bioactive compounds into food to improve its functionality (Gleeson, Ryan, & Brayden, 2016). Nevertheless, O/W emulsions are thermodynamically unstable, so they tend to break down over time (McClements, 2015). Thus, one of the most important challenges to be faced in their formulation is to guarantee their long-term colloidal stability, which can be achieved by the proper selection of the emulsifier. A wide range of emulsifiers have been already reported to be useful for the successful formation and stabilization of O/W emulsions, being small molecule surfactants and protein the most studied (Kralova & Sjöblom, 2009; Molet-Rodríguez, Salvia-Trujillo, & Martín-Belloso, 2018). Nowadays, there is a need to re-evaluate by-products or residues from the food chain with the potential to become new ingredients. In this context, pectin, a heteropolysaccharide found in the primary cell wall of fruits and vegetables has been shown to effectively contribute to the emulsification and stabilization of O/W emulsions (Chandel et al., 2022; Christiaens et al., 2015; Dickinson, 2009). In general, pectin structure consists of three main domains: homogalacturonan (HG), rhamnogalacturonan I (RG-I), and rhamnogalacturonan II (RG-II), with HG and RG-I accounting for approximately 60–65% and 20–35% of the total pectin content of plant tissues,

* Corresponding author. Department of Food Technology, University of Lleida, Av. Alcalde Rovira Roure 191, 25198, Lleida, Spain.
E-mail addresses: anna.molet@udl.cat (A. Molet-Rodríguez), daamendezre@unal.edu.co (D.A. Méndez), amparo.lopez@iata.csic.es (A. López-Rubio), mjfabra@iata.csic.es (M.J. Fabra), marta.martinez@csic.es (M. Martínez-Sanz), laura.salvia@udl.cat (L. Salvia-Trujillo), olga.martin@udl.cat (O. Martín-Belloso).

https://doi.org/10.1016/j.foodhyd.2024.110553
Received 22 May 2024; Received in revised form 14 August 2024; Accepted 19 August 2024
Available online 24 August 2024

respectively (Alba & Kontogiorgos, 2017; Assifaoui, Hayrapetyan, Gallery, & Agoda-Tandjawa, 2024; Ngouémazong, Christiaens, Shpigelman, Van Loey, & Hendrickx, 2015). HG domain consists of a linear backbone composed of galacturonic acid (GalA) monomer units, which can be naturally methyl-esterified or acetylated. Rhamnogalacturonan I (RG-I) is a branched and structurally heterogeneous domain characterized by a long sequence of alternating GalA and rhamnose (Rha) residues, in which Rha can be substituted by neutral sugar side chains composed of arabinose (Ara) and galactose (Gal). The ratio between (Ara + Gal)/Rha determines the degree of branching of each pectin. Apart from polysaccharides, the primary cell wall of plants contains structural proteins, which are also present in pectin extracts preferentially bound to neutral sugar side chains of pectin (Alba & Kontogiorgos, 2017; Caffall & Mohnen, 2009). Studies carried out mainly on apple, citrus and sugar beet pectin have demonstrated that the emulsifying properties of pectin are related to its chemical composition, molecular structure and conformation. Hydrophobic moieties (e.g. protein, acetyl and ferulic acid), degree of esterification (DE), molecular weight (M_w) and degree of branching of pectin are highly associated with its ability to adsorb at the oil-water interface and stabilize O/W emulsions (Funami et al., 2007; Humerez-Flores, Verkempinck, Van Loey, Moldenaers, & Hendrickx, 2022; Leroux, Langendorff, Schick, Vaishnav, & Mazoyer, 2003; Niu, Chen, Luo, Chen, & Fu, 2022; Schmidt et al., 2015; Shuai et al., 2022; Siew, Williams, Cui, & Wang, 2008; Verkempinck et al., 2018). Nevertheless, these structural characteristics are well-known to vary depending on the sources where it is extracted and also on the extraction methods. Lately, some authors have shown that persimmon pectin also exhibits a promising emulsifying potential, yet its emulsification mechanisms are still poorly understood (Jia, Du, Li, & Li, 2022; Jia, Khalifa, et al., 2022; Jiang, Xu, Li, Li, & Huang, 2020; Luo et al., 2014). In a previous study, the modification of extraction conditions (pH and temperature) has been shown to influence the structural characteristics of pectin extracts from persimmon waste (Méndez et al., 2022). First, increasing the severity of the extraction conditions resulted in a reduction of the degree of methyl esterification of pectin. Second, the content of structural neutral sugars, GalA and Rha, increased and remained constant, respectively, with incrementing the severity of extraction. Moreover, Ara was only present in the pectin extract obtained using low severity of extraction, whereas Gal content was similar using low, medium and high extraction conditions. Thus, the degree of branching in pectin was higher when low-severe extraction conditions were used in comparison with higher severity. Last, pectin interaction with polyphenols differed between extracts because of these structural and compositional changes of pectin when using varying extraction severities. Low severity conditions led to high amounts of non-covalently and covalently linked phenolics, medium severity conditions led to mainly non-covalently linked phenolics and few covalently linked phenolics and the high severity conditions led to low amounts of both non-covalently linked phenolics. Regarding the internal composition of polyphenols, benzoic acids, mainly gallic acid, protocatechuic acid and vanillin, were the major constituents in all extracts.

The main aim of this work was to study the influence of pectin structural characteristics and its interactions with polyphenols, on the emulsification properties of pectin extracts from persimmon waste at pH 3 or 7. Specifically, three pectin-rich extracts with different pectin-polyphenol interactions, being free phenolics-extract (FP-E), covalent phenolics-extract (CP-E) and non-covalent phenolics-extract (NCP-E), were obtained using varying severity extraction conditions. First, pectin extracts were characterized in terms of thermal properties, electrical charge, molecular structure and nanostructural conformation. After that, their interfacial properties were evaluated in terms of interfacial layer thickness and dynamic interfacial tension. Moreover, O/W emulsions stabilized with each persimmon pectin extract were formed and their physicochemical properties and colloidal stability were analyzed after formation and during storage at 4 °C.

2. Material and methods

2.1. Materials

Medium-chain triglyceride oil (Miglyol® 812 N) with a purity of 99.9%, according to its certificate of analysis, from IOI Oleochemical GmbH (Hamburg, Germany) was used in the dynamic interfacial tension measurement. Corn oil (Koipesol Asua, Deoleo, Spain) was the lipid phase selected for the formation of O/W emulsions. Immature persimmon fruit (Diospyros kaki Thunb) "Rojo brillante-Ribera del Xuquer" was kindly supplied by Anecoop S. Coop., during the autumn season of 2021 in Spain. Aqueous suspensions of 10% (w/v) melamine fluoride (MF) or 5% (w/v) polystyrene (PS) microspheres were purchased from Microparticles GmbH (Berlin, Germany). Sodium azide was from Fischer Scientific (Loughborough, UK). The rest of the chemicals used were of analytical grade. All persimmon pectin aqueous solutions or O/W emulsions were prepared with Milli-Q water with a resistivity of 18.2 MΩ cm at 25 °C (Milli-Q apparatus, Millipore, Bedford, UK).

2.2. Methods

2.2.1. Persimmon pectin extraction

Immature persimmon fruits were processed removing the calix and peduncle, cut into pieces of around 0.5–2.5 cm and stored in protective bags at - 20 °C. Then, persimmon pectin extracts were obtained using the following extraction conditions with increased severity in terms of combination of acidity and temperature: low severity (pH 1.5, 70 °C), medium severity (pH 1, 95 °C) or high severity (pH 0.5, 82.5 °C), according to a previous study (Méndez et al., 2022). These extraction conditions led to differences in chemical composition, structure, conformation and as a consequence pectin-polyphenol interactions. Thus, in the present study, persimmon pectin extracts obtained using low, medium and high severity conditions will be named along the manuscript as covalent phenolics-extract (CP-E), non-covalent phenolics-extract (NCP-E), free phenolics-extract (FP-E), respectively. Their main structural characteristics as well as the composition of neutral sugar and GalA are shown in Table 1 and Supplementary Material Table S1, respectively.

2.2.2. Characterization of the persimmon pectin extracts

2.2.2.1. Thermal properties. The thermal properties of the three persimmon pectin extract powders were evaluated through differential scanning calorimetry (DSC), in triplicate, using a TA Instrument (New Castle, DE, USA) thermal analysis system under nitrogen atmosphere. The analysis was carried out on 3 mg of each sample at a heating rate of 10 °C/min, from 25 °C to 500 °C.

2.2.2.2. ζ -potential. Persimmon pectin extract aqueous solutions were prepared by dissolving 1% (w/w) of each pectin extract in Milli-Q water and kept under magnetic stirring (360 rpm) overnight. Then, the pH of each pectin aqueous solution was adjusted to values between 3 and 7. Persimmon pectin extract aqueous solutions were further diluted 1:100 in Milli-Q water and posteriorly set again at the corresponding pH. The ζ-potential was measured by phase-analysis light scattering (PALS) by using a Zetasizer NanoZS laser diffractometer.

2.2.2.3. Molecular structure and nanostructural conformation

2.2.2.3.1. Hydrodynamic diameter. The hydrodynamic diameter of the different persimmon pectin extracts in aqueous solution at pH 3 or 7 was measured, according to the procedure described by Schmidt, Schütz, and Schuchmann (2017) and Verkempinck et al. (2018). Persimmon pectin extracts aqueous solutions (0.25% w/w) were prepared in Milli-Q water and kept under magnetic stirring (360 rpm) overnight to allow their hydration. Afterwards, the pectin solutions were

Table 1
Structural characteristics of the three persimmon extracts.

Extract	Severity of extraction	DE (%)[a]	Branching[b]	Total phenolics (mg/kg)		
				Free	Esterified[c]	Conjugated[d]
FP-E	High (pH 0.5, 82.5 °C)	54.5 ± 0.44	2.07	1013	111	128
NCP-E	Medium (pH 1, 95 °C)	62.91 ± 1.7	2.31	1889	346	698
CP-E	Low (pH 1.5, 70 °C)	74.24 ± 0.74	5.32	1814	4607	1264

Data from Méndez et al. (2022).
Free phenolics-extract (FP-E), non-covalent phenolics-extract (NCP-E) and covalent phenolics-extract (CP-E).
[a] Degree of esterification (DE).
[b] (Gal + Ara)/Rha ratio was used as an indicator of pectin branching.
[c] corresponding to phenols recovered in the alkali fraction.
[d] corresponding to phenols recovered in the acid fraction.

diluted further to yield samples with concentrations ranging from 0.01 to 0.25% (v/v) and adjusted to pH 3 or 7 using HCl (0.1 or 1 M) or NaOH (0.1 or 1M). These solutions were given another 2 h for hydration. Then, they were further diluted 1:1 in Milli-Q water, adjusted at the corresponding pH (3 or 7) and measured in terms of average particle size using a Zetasizer NanoZS laser diffractometer (Malvern Instruments Ltd., Worcestershire, UK). The detected particle size was plotted against the corresponding concentration of persimmon pectin extract aqueous solution and extrapolated to zero to obtain the hydrodynamic diameter of each persimmon pectin extract at a certain pH.

2.2.2.3.2. Small angle X-ray scattering (SAXS). SAXS experiments were carried out in the Non-Crystalline Diffraction beamline, BL-11, at ALBA synchrotron light source (www.albasynchrotron.es). Persimmon pectin extracts aqueous solutions (2% w/w) were prepared in Milli-Q water and were placed in sealed 2 mm quartz capillaries (Hilgenberg GmbH, Germany). The energy of the incident photons was 12.4 KeV or equivalently a wavelength, λ, of 1 Å. The SAXS diffraction patterns were collected by means of a photon counting detector, Pilatus 1M, with an active area of 168.7 × 179.4 mm^2, an effective pixel size of 172 × 172 μm^2 and a dynamic range of 20 bits. The sample-to-detector distance was set to 7570 mm, resulting in a q range with a maximum value of q = 0.19 $Å^{-1}$. An exposure time of 10 s was selected based on preliminary trials. The data reduction was treated by pyFAI python code (ESRF) (Kieffer & Ashiotis, 2014), modified by ALBA beamline staff, to do on-line azimuthal integrations from a previously calibrated file. The calibration files were created from a silver behenate (AgBh) standard. The intensity profiles were then represented as a function of q using the IRENA macro suite (Ilavsky & Jemian, 2009) within the Igor software package (Wavemetrics, Lake Oswego, Oregon).

The obtained scattering patterns were properly described using a two-level unified model. Such model considers that, for each individual level, the scattering intensity is the sum of a Guinier term and a power-law function (Beaucage, 1995, 1996):

$$I(q) = \sum_{i=1}^{N} G_i \exp\left(-q^2 \bullet \frac{R_{g.i}^2}{3}\right) + \frac{B_i\left[erf\left(qR_{g.i}/\sqrt{6}\right)\right]^{3P_i}}{q^{P_i}} + bkg \quad (1)$$

where $G_i = c_i V_i \Delta SLD_i^2$ is the exponential prefactor (where V_i is the volume of the particle and ΔSLD_i is the scattering length density (SLD) contrast existing between the i^{th} structural feature and the surrounding solvent), $R_{g.i}$ is the radius of gyration describing the average size of the i^{th} level structural feature, B_i is a q-independent prefactor specific to the type of power-law scattering with power-law exponent, P_i, and *bkg* is the background. In this case, the largest structural level was modelled only by a power-law (R_{g1} was fixed at a value $\gg q_{min}^{-1}$ of 5000 Å).

The obtained values from the fitting coefficients are those that minimize the value of Chi-squared, which is defined as:

$$\chi^2 = \sum \left(\frac{y - y_i}{\sigma_i}\right)^2 \quad (2)$$

where y is a fitted value for a given point, y_i is the measured data value for the point and σ_i is an estimate of the standard deviation for y_i. The curve fitting operation is carried out iteratively and for each iteration, the fitting coefficients are refined to minimize χ^2.

2.2.3. Interfacial properties of the persimmon pectin extracts

2.2.3.1. Interfacial layer thickness. The interfacial layer thickness of persimmon pectin extracts to both polystyrene (PS) and melamine fluoride (MF) microspheres was measured to investigate the possible pectin organization at a droplet surface. MF was positively charged, whereas PS microspheres were negatively charged. Briefly, persimmon pectin extract aqueous solutions (2% w/w) in Milli-Q water were prepared and stirred at 360 rpm overnight. Then, the pH of each persimmon pectin solution was set at pH 3 and 7. In parallel, solutions of MF or PS (0.5% v/v) in Milli-Q water were prepared and adjusted at pH 3 and 7. Then, persimmon pectin solutions were mixed (1:1) with 0.5% (v/v) microspheres at 200 rpm as described by Schmidt et al. (2017). The particle size of this mixture was smeasured using the Zetasizer NanoZS laser diffractometer with a dilution of 1:100 in Milli-Q water and the adjustment of the corresponding pH. MF and PS microspheres had a known particle size of 465 ± 40 and 460 ± 10 nm, respectively. Finally, the adsorbed layer thickness was calculated from the difference in size between the adsorbed and non-adsorbed microspheres.

2.2.3.2. Dynamic interfacial tension. Persimmon pectin aqueous solutions (0.01 % w/w) in Milli-Q water were prepared and kept under magnetic stirring (360 rpm) overnight. Then, the pH of the previously prepared solutions was set to 3 and 7. A drop shape analysis system DSA25 (KRÜSS, Hamburg, Germany) was used to evaluate the change in interfacial tension (IFT; mN/m) caused by persimmon pectin solutions at pH 3 or 7. A droplet of MCT oil was formed at the tip of a U-shaped needle, while the persimmon pectin aqueous solutions were located in a cuvette. The pendant drop measurements recording the changes of the IFT were performed for 2 h.

2.2.4. Emulsification properties of the persimmon pectin extracts

2.2.4.1. Formation of the O/W emulsions. Firstly, persimmon pectin solutions (1% w/w) were prepared in Milli-Q water and kept under magnetic stirring (360 rpm) overnight to allow their hydration. Then, coarse O/W emulsions were prepared by pre-homogenizing 2% (w/w) of corn oil with 98% w/w of each persimmon pectin solution, using a high shear laboratory mixer, T-25 digital Ultra-Turrax (IKA, Staufen, Germany), working at 7200 rpm for 3 min. Then, O/W emulsions with oil droplets in the submicron range were obtained by passing the coarse O/W emulsions two times through an LM10 Microfluidizer (Microfluidics, Westwood, MA, USA) at a pressure of ~130 MPa. The native pH values of the O/W emulsions stabilized with FP-E, CP-E and NCP-E were 3.3, 3.1 and 2.9, respectively. The pH of the O/W emulsions was adjusted to pH 3 and 7 by using NaOH or HCl (0.1 or 1M). Finally, sodium azide (0.02% w/w) was added to all the O/W emulsions as a preservative.

2.2.4.2. Physico-chemical properties of O/W emulsions

2.2.4.2.1. Particle size and size distribution. Particle size and size distribution of the O/W emulsions were determined by dynamic light scattering (DLS), using a Zetasizer NanoZS laser diffractometer, with a dilution of 1:100 in Milli-Q water and the posterior adjustment of the pH to 3 or 7. The average particle size and size distribution were reported as z-average (nm) and intensity (%), respectively. The refractive indexes for corn oil and Milli-Q water were 1.47 and 1.33, respectively.

2.2.4.2.2. ζ-potential. The ζ-potential (mV) of the O/W emulsions was determined by phase-analysis light scattering (PALS) with a Zetasizer NanoZS laser diffractometer. O/W emulsions were prior diluted in Milli-Q water with a dilution factor of 1:100 aliquot-to-solvent and their pH was adjusted to 3 or 7.

2.2.4.2.3. Optical microscopy analysis. Phase contrast microscopy images of the samples were taken with an optical microscope (BX41, Olympus, Göttingen, Germany) using a 100x oil immersion objective lens and equipped with UIS2 optical system. All images were processed using the instrument software (Olympus cellSense, Barcelona, Spain).

2.2.4.2.4. Colloidal stability of O/W emulsions. The colloidal stability of the O/W emulsions was determined by measuring the average particle size and visually monitored by phase contrast microscopy and visual images during 20 days of storage at 4 °C.

2.3. Statistical analysis

All experiments were assayed in duplicate unless otherwise specified, and data was expressed as the mean with standard deviation. An analysis of variance was carried out and the Tukey HSD test was run to determine significant differences at a 5% significance level ($p < 0.05$) with statistical software JMP Pro 14 (SAS Institute Inc.).

3. Results and discussion

3.1. Visual appearance of the persimmon pectin extracts

Colour differences were visually observed among the three different pectin extracts in aqueous solution. FP-E aqueous solutions appeared orange/brown-coloured, NCP-E solutions were orange/pink-coloured and CP-E solutions were mainly pink (Fig. 1). FP-E is composed mainly of free pectin and polyphenol molecules, while NCP-E and CP-E had high quantities of polyphenols linked with pectin molecules, yet being non-covalent and covalent interactions, respectively. Thus, both the amount of pectin interacting with polyphenols and the type of interactions seemed to influence the optical properties of pectin extracts in aqueous solution. Regarding the visual appearance of each persimmon pectin aqueous solution at different pH values ranging from 3 to 7, colour changes were observed when increasing the pH above to 5 for all the pectin aqueous solutions (Fig. 1). Polyphenols are well-known to experience variations in their colour at different pH values, which has been attributed to degradation or chemical modifications (Friedman & Jürgens, 2000). Thus, this would explain the colour changes observed for the pectin aqueous solutions when increasing the pH up to 5. In particular, the colour of the CP-E was maintained even at pH 6 and changes were observed up to pH 7. This indicates that the covalent interactions between polyphenol and pectin molecules result in colour stabilization, as these interactions are probably hindering either degradation or structure modification (Jakobek & Matić, 2019).

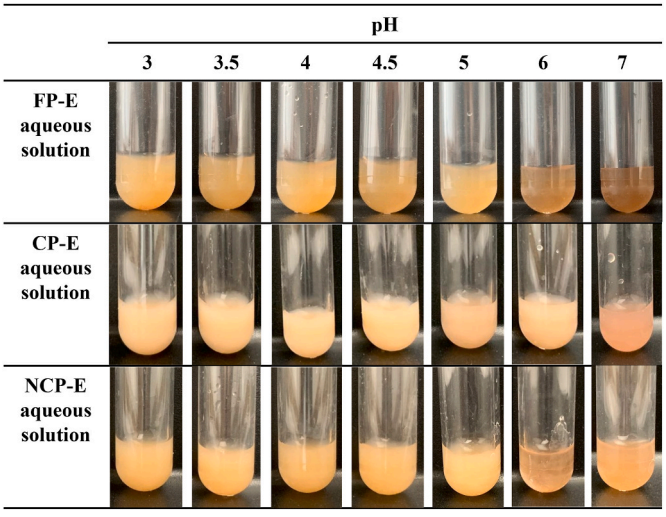

Fig. 1. Visual appearance of persimmon pectin extracts in aqueous solution (1% w/w) differing in polyphenol-pectin interactions, being free phenolics rich-extract (FP-E), covalent phenolics rich-extract (CP-E) and non-covalent rich phenolics-extract (NCP-E) at pH ranging from 3 to 7.

3.2. Characterization of the persimmon pectin extracts

3.2.1. Thermal properties

DSC was used to determine the thermal properties of the different pectin extracts, obtained under three different extraction conditions. According to Fig. 2, the endothermic peak ascribed to the melting transition phase was found at around 152 °C for CP-E, whereas it occurred at higher temperatures for FP-E (~184 °C) and NCP-E (~186 °C). These results were consistent with those reported by other authors who found the melting temperature of dried pectins between 150 and 200 °C, which was explained by a phase transition from a crystalline to an amorphous structure (Iijima, Nakamura, Hatakeyama, & Hatakeyama, 2000; Osorio, Carriazo, & Barbosa, 2011; Pereira, Carmello-Guerreiro, & Hubinger, 2009). Interestingly, the presence of a higher amount of covalently bound polyphenols (CP-E) significantly decreased the thermal transition of pectin, thus indicating that smaller or more imperfect crystallites were formed in this case, which is also supported by the higher degree of branching (lower linearity) compared to the other samples (Branching degree: 5.32 CP-E, 2.07 FP-E, 2.31 NCP-E), thus resulting in a slightly amorphous structure of the pectin. On the other hand, NCP-E displayed a very significant reduction in esterified phenolics, which are probably hindering the proper packing of the carbohydrate chains.

The exothermic transitions observed around 230 °C for the three pectin extracts correspond to pectin degradation and, although very similar between them, a slightly higher degradation temperature was observed for CP-E, thus suggesting that covalently bound polyphenols can result in higher thermal stability that it can be also influenced by the

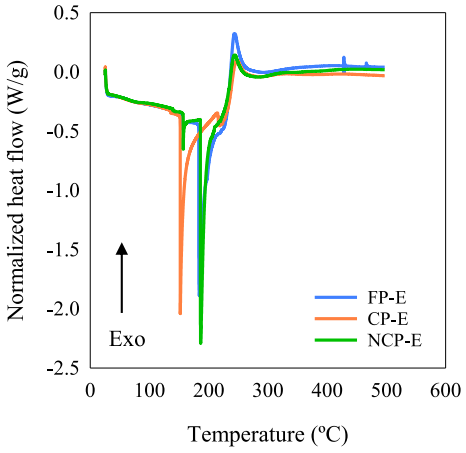

Fig. 2. Differential scanning calorimetry (DSC) curves of persimmon pectin extracts powder differing in polyphenol-pectin interactions, being free phenolics rich-extract (FP-E), covalent phenolics rich-extract (CP-E) and non-covalent rich phenolics-extract (NCP-E).

presence of branched zones. The degradation temperatures observed were in the range of others found in the scientific literature for pectin (Dranca, Vargas, & Oroiana, 2020; Wang, Chen, & Lü, 2014).

3.2.2. ζ-potential

In general, the ζ-potential of persimmon pectin aqueous solutions became more negative as the pH increased from 3 to ~5 (Fig. 3). Pectin is an acidic heteropolysaccharide rich in galacturonic units, which contains a carboxyl group (-COOH) at the C-6 with a dissociation constant (pK_a) of around 3.5 and 4.5 (Einhorn-Stoll, Kastner, Hecht, Zimathies, & Drusch, 2015). Increasing the pH of pectin extract solutions above the pK_a of pectin molecules would result in an increased number of dissociated carboxyl groups in their galacturonic units, explaining the more negative ζ-potential values obtained for all the persimmon pectin solutions as the pH was increased from 3 to around 5 (Humerez-Flores et al., 2022; Verkempinck et al., 2018). From pH 5 onwards, there were no significant differences in the ζ-potential values of each pectin extract in aqueous solution due to pH increase. Regarding the differences in pectin structural characteristics and its interactions with polyphenols, it did not affect the ζ-potential when the pH was between 3 and 4, yet at higher pH values CP-E and NCP-E had less negative electrical charges in comparison with FP-E, even no significant differences were found. For instance, at pH 5, FP-E showed more negative electrical charge (−67.44 ± 1.24 mV) than CP-E and NCP-E (−54.67 ± 8.82 and −56.93 ± 3.48 mV, respectively) (Fig. 3). This less negative electrical charges for CP-E and NCP-E compared to FP-E could be explained by less dissociated carboxyl groups in their galacturonic units, which could be methyl esterified. In fact, the DE of FP-E, NCP-E and CP-E were 54.5 ± 0.44, 62.91 ± 1.7 and 74.24 ± 0.74%, respectively (Table 1). Moreover, carboxyl groups of pectin galacturonic acid could also be interacting with polyphenols either covalently or non-covalently.

3.2.3. Molecular structure and nanostructural conformation

3.2.3.1. Hydrodynamic diameter. The hydrodynamic diameter of persimmon pectin in aqueous solutions varied among extracts and with pH. FP-E had a smaller hydrodynamic diameter compared to CP-E and NCP-E. For instance, at pH 3, FP-E had a hydrodynamic diameter of 539.92 ± 113.58 nm, while it was 1532.70 ± 3.68 and 1089.50 ± 77.50 nm for CP-E and NCP-E, respectively (Table 2). In general, it has been reported that the lower the DE, the more negative electrical charges, which led to more expanded conformation due to pectin chain repulsion (Morris, Foster, & Harding, 2000; Schmidt et al., 2017; Verkempinck et al., 2018). In the present study, the DE of pectin extracts decreased when increasing extraction severity (DE: CP-E > NCP-E > FP-E) (Table 1). Thus, in contrast with other published studies, pectin with the lowest DE (FP-E) had the lowest hydrodynamic diameter in solution. In this regard, results from the present work showed a relationship between the interactions of pectin with polyphenols and its hydrodynamic diameter, with CP-E and NCP-E leading to bigger structures in aqueous solution compared to FP-E. This would mean that free polyphenols in the pectin extracts would not contribute to the volume of the pectin hydrocolloid in solution, while when polyphenols are covalently or non-covalently bound to pectin they contribute to their overall hydrocolloid volume. In this regard, it has been previously reported that pectin can reorganize forming hydrophobic pockets in its structure able to encapsulate polyphenols, whose presence could cause changes in the pectin structure, explaining its increased hydrodynamic diameter (Le Bourvellec, Bouchet & Renard, 2005). Interestingly, this increase in size was more accentuated for pectin extracts with high amounts of covalently bound polyphenols, as in CP-E, than non-covalently bound ones (NCP-E). Apart from that, the higher hydrodynamic diameters observed for CP-E and NCP-E in comparison with FP-E could also be explained by their higher branching degree, which is expected to result in pectin with more expanded conformation and bigger size than pectin with low branching degrees (Table 1). Nevertheless, the relationship between pectin branching degree and its size and conformation is still unclear, since an increase in pectin branching has also been shown to result in more flexibility, compactness and smaller size than when it has mainly linear domains (Cui et al., 2020; Santiago et al., 2018). Finally, it could also be possible that increasing the severity of extraction would have resulted in lower M_w pectin, explaining the smaller sizes of FP-E in comparison with CP-E and NCP-E.

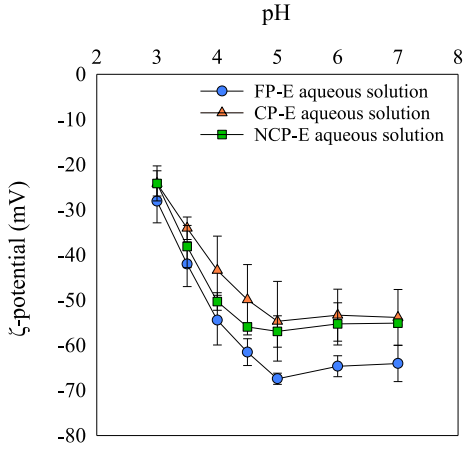

Fig. 3. ζ-potential values (mV) of persimmon pectin extracts in aqueous solution (1% w/w) differing in polyphenol-pectin interactions, being free phenolics-extract (FP-E), covalent phenolics-extract (CP-E) and non-covalent phenolics-extract (NCP-E) at pH ranging from 3 to 7.

Table 2
Hydrodynamic diameter (nm) of persimmon pectin extracts in aqueous solution differing in polyphenol-pectin interactions, being free phenolics-extract (FP-E), covalent phenolics-extract (CP-E) and non-covalent phenolics-extract (NCP-E), measured at pH 3 and 7. A,B letters mean significant differences between different formulations for the same pH. a,b letters indicate significant differences between different pH for the same formulation.

	Hydrodynamic diameter (nm)	
	pH 3	pH 7
FP-E aqueous solution	539.92 ± 113.58^{Ca}	781.55 ± 57.96^{Ba}
CP-E aqueous solution	1532.70 ± 3.68^{Ab}	1791.40 ± 5.23^{Aa}
NCP-E aqueous solution	1089.50 ± 77.50^{Ba}	1092.20 ± 122.47^{Ba}

CP-E showed a significantly bigger hydrodynamic diameter at pH 7 (1791.40 ± 5.23 nm) than at pH 3 (1532.70 ± 3.68 nm). Similarly, a bigger hydrodynamic diameter was also observed for FP-E at pH 7 (781.55 ± 57.96 nm) than at pH 3 (539.92 ± 113.58 nm), yet without significant differences. As mentioned earlier, carboxyl groups in pectin galacturonic units have a pK_a of around 3.5 and 4.5. At pH 7, which is above the pK_a, carboxyl groups are mainly ionized, resulting in inter- and intramolecular repulsion and consequently leading to a more expanded molecular structure. Similar to our results, other authors have shown that the hydrodynamic diameter of sugar beet or citrus pectin in aqueous solution increased with the pH (Bindereif, Karbstein, Zahn, & van der Schaaf, 2022; Schmidt et al., 2017; Verkempinck et al., 2018).

3.2.3.2. Small angle X-ray scattering. To further investigate the nanostructural conformation of the pectin chains in aqueous solutions, SAXS experiments were carried out on aqueous solutions of the extracts and the obtained scattering patterns are shown in Fig. 4. As evidenced by the Kratky plots (Fig. 4B), the NCP-E and FP-E extracts presented similar patterns, where a broad shoulder feature was detected within the low-q region ($q < 0.03$ Å^{-1}). This feature has been previously detected in some pectin solutions at conditions at which some degree of clustering took place as a result of molecular interactions (Méndez et al., 2021; Méndez,

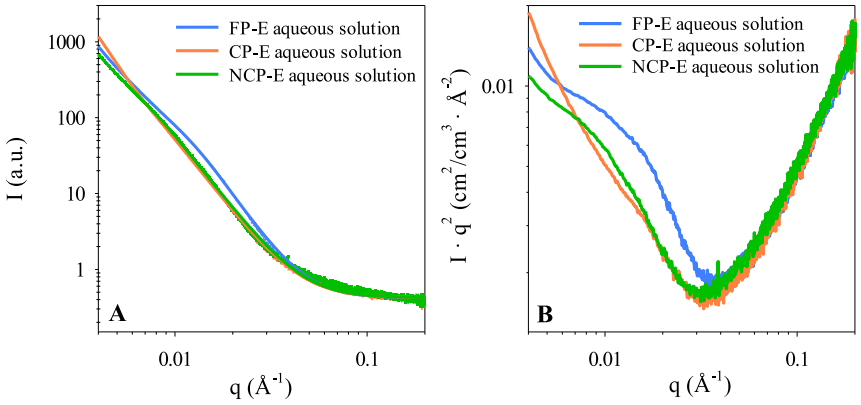

Fig. 4. (A) Small angle X-ray scattering (SAXS) patterns from persimmon pectin extracts in aqueous solution (2% w/w) and (B) their corresponding Kratky plots. In (A) markers represent the experimental data and solid lines show the fits obtained using the Beaucage model.

Martínez-Abad, Martínez-Sanz, López-Rubio, & Fabra, 2023). The fact that this feature was not visible in CP-E might be originated by a greater interfacial scattering length density contrast between the polymeric chains and the surrounding solvent, as a result of the higher amount of covalently bound polyphenols in that case. The inherent presence of polyphenols may affect the scattering length density of the polymeric chains, but it could also affect the packing density. The fitting results evidenced the presence of surface fractal structures (power-law exponents $P_2 = 3.2–3.6$), which arose from the surface scattering of the rough particles formed by pectin chain clusters. The values obtained for the radii of gyration (Rg_2) were 52.9 nm for NCP-E, 57.9 nm for CP-E and 31.4 nm for FP-E. This, in line with the determined hydrodynamic diameter, indicates that larger intermolecular distances were found when polyphenols were bound to the pectin chains, as in NCP-E and CP-E.

3.3. Interfacial properties of the persimmon pectin extracts

3.3.1. Interfacial layer thickness

In general, the interfacial layer thickness of the persimmon pectin extracts once absorbed into MF or PS microspheres was thicker at pH 3 than at pH 7. For instance, the interfacial layer thickness of FP-E adsorbed in MF microspheres was 479.73 ± 12.95 and 314.20 ± 38.63 nm when its aqueous solution was at pH 3 and 7, respectively (Table 3). This may be attributed to the fact that at pH 3, pectin molecules had a folded and compact conformation (see section 3.2.3.1), rendering thick interfacial layers. Moreover, at this pH, pectin molecules could be adsorbing at interfaces in multilayers, as electrostatic repulsion between them is weakened due to the almost neutral carboxyl groups, whereas hydrogen bonds and hydrophobic interactions are strengthened (Niu et al., 2022). Instead, unfolded pectin conformation, as a result of electrostatic repulsions between highly negatively charged carboxyl groups from pectin chains at pH 7, would adsorb flat and without multilayer formation, resulting in thinner interfacial layers than pectin molecules at pH 3. Similarly, other authors have reported a thicker interfacial layer for sugar beet, apple and citrus pectin at pH 3 in comparison with pH 7 (Bindereif et al., 2022; Niu et al., 2022; Siew et al., 2008; Verkempinck et al., 2018). Regarding the effect of polyphenol-pectin interactions, there were no significant differences between the interfacial layer thickness of the different pectin extracts at pH 7 once absorbed into the microspheres (Table 3). Nevertheless, at pH 3, NCP-E presented a thicker interfacial layer thickness at the microspheres than FP-E or CP-E, suggesting that pectin structural characteristics and/or its interactions with polyphenols can influence its organization at interfaces.

Table 3
Interfacial layer thickness (nm) of persimmon pectin extracts in aqueous solution differing in polyphenol-pectin interactions, being free phenolics-extract (FP-E), covalent phenolics-extract (CP-E) and non-covalent phenolics-extract (NCP-E), onto polystyrene (PS) and melamine fluoride (MF) microspheres, measured at both pH 3 and 7. A,B letters mean significant differences between different formulations for the same pH and microspheres. a,b letters indicate significant differences between different pH for the same formulation and microsphere. x,y letters indicate significant differences between different microspheres for the same pH and formulation.

	Interfacial layer thickness (nm)			
	pH 3		pH 7	
	MF	PS	MF	PS
FP-E aqueous solution	479.73 ± 12.95^{Bax}	230.82 ± 5.75^{Bay}	314.20 ± 38.63^{Abx}	142.38 ± 25.43^{Abx}
CP-E aqueous solution	465.77 ± 8.74^{Bax}	480.80 ± 129.42^{ABax}	312.76 ± 15.59^{Abx}	115.01 ± 11.28^{Aay}
NCP-E aqueous solution	562.98 ± 14.18^{Aax}	663.01 ± 60.56^{Aax}	311.33 ± 15.31^{Abx}	170.67 ± 1.25^{Aby}

MF were positively charged, whereas PS microspheres were negatively charged.

3.3.2. Dynamic interfacial tension

All persimmon pectin aqueous solutions were able to decrease the IFT of the MCT oil droplet from 35 to at least 25 mN/m, evidencing their ability to adsorb at the oil-water interface, regardless of the pectin-polyphenol interactions and pH (Fig. 5). Nevertheless, there were some differences in their IFT decay during time and end-point. At pH 7, no differences in the effectiveness of decreasing the IFT during time or after 120 min were observed between the different persimmon pectin aqueous solutions (Fig. 5). In contrast, at pH 3, FP-E was faster in decreasing the oil droplet IFT and reached lower final values in comparison with CP-E and NCP-E. FP-E was able to reach IFT values below 16 mN/m after 40 min in contact with the MCT oil droplet, whereas, at the same time, CP-E and NCP-E could only achieve IFT values above 20 mN/m (Fig. 5). In addition, after 120 min, FP-E reached IFT values of 13.89 ± 1.07 mN/m, whereas CP-E and NCP-E had values of 20.08 ± 0.52 and 22.55 ± 0.26 mN/m, respectively. Thus, at pH 3, structural characteristics, conformation in solution and covalent or non-covalent interactions between pectin and polyphenols decreased the ability of pectin to absorb at the oil/water interface and consequently its ability to reduce the IFT between both liquids. Moreover, it has been also reported that polyphenols can act as surface-active molecules, helping in decreasing the oil droplet IFT when being free as in the case of FP-E (Di Mattia, Sacchetti, Mastrocola, Sarker, & Pittia, 2010; Velderrain-Rodríguez, Salvia-Trujillo, González-Aguilar, & Martín-Belloso, 2021).

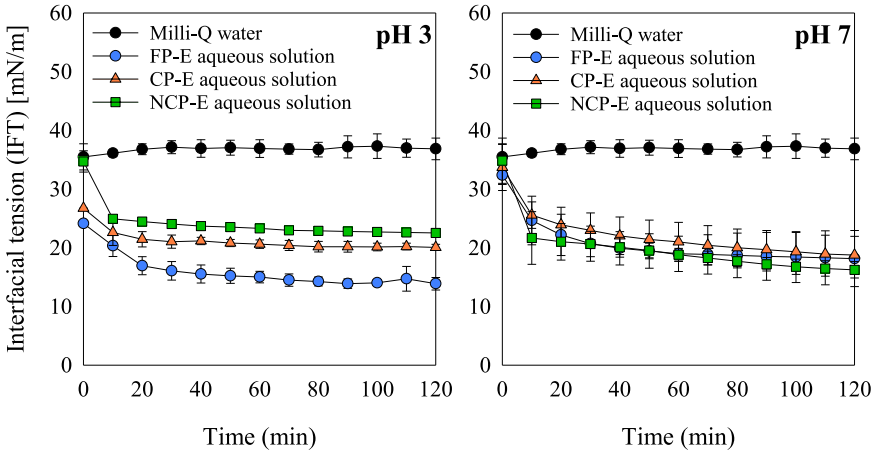

Fig. 5. Interfacial tension (IFT) [mN/m] of persimmon pectin extracts in aqueous solution (0.01% w/w) differing in polyphenol-pectin interactions, being free phenolics-extract (FP-E), covalent phenolics-extract (CP-E) and non-covalent phenolics-extract (NCP-E), measured at pH 3 and 7.

3.4. Emulsification properties of the persimmon pectin extracts

3.4.1. Physicochemical properties of O/W emulsions immediately after preparation

The initial visual appearance of the O/W emulsions showed differences in colour depending on the persimmon pectin extract used to stabilize them. FP-E and NCP-E-stabilized O/W emulsions appeared brown-coloured, whereas the CP-E-stabilized O/W emulsion was pink-coloured (Fig. 6). Nevertheless, all the O/W emulsions appeared homogenous, meaning that they were stable immediately after formation. Indeed, all O/W emulsions had a monomodal size distribution with submicron oil particle sizes (Fig. 7 and Table 4). Similar particle sizes for O/W emulsions stabilized with persimmon pectin have been reported by other authors, evidencing the emulsifying ability of persimmon pectin (Jia et al., 2022a, 2022b). There were no significant differences between the particle size of FP-E, CP-E or NCP-E stabilized O/W emulsions immediately after preparation. At pH 3, FP-E, CP-E and NCP-E stabilized O/W emulsions showed average particle sizes of 532.40 ± 28.57, 402.63 ± 41.27 and 549.38 ± 77.75 nm, respectively, whereas, at pH 7, they had average particle size values of 656.13 ± 46.72, 505.80 ± 67.06 and 569.05 ± 5.35 nm, respectively (Table 4). Despite the absence of differences in the particle size of the O/W emulsions formulated with the different persimmon pectin extracts, changes were observed in their microstructure. At pH 3, phase contrast microscopy images of both FP-E and NCP-E-stabilized O/W emulsions immediately after preparation showed particle aggregation, which was not present in the CP-E stabilized O/W emulsions (Fig. 8). It suggests that FP-E or NCP-E promote depletion flocculation of oil droplets of the O/W emulsion. This mechanism can occur when there is a high concentration of non-adsorbed polysaccharide, such as pectin, in aqueous phase that causes droplets to pull together by osmotic pressure. Thus, free or non-covalently linked polyphenols can result in a higher concentration of pectin in the bulk aqueous phase that would cause depletion flocculation and finally aggregation of the oil droplets in FP-E or NCP-E-stabilized O/W emulsions. This aggregation was less present or absent at pH 7 (Fig. 9), probably because of the higher repulsive forces between the oil droplets at pH > pK_a, as they presented more negative ζ-potential values than at pH 3. O/W emulsions formulated with persimmon pectin aqueous solutions at pH 3 had ζ-potential values between −16 and −22 mV yet increasing the pH to 7 led to ζ-potential values more negative than −49 mV (Table 4).

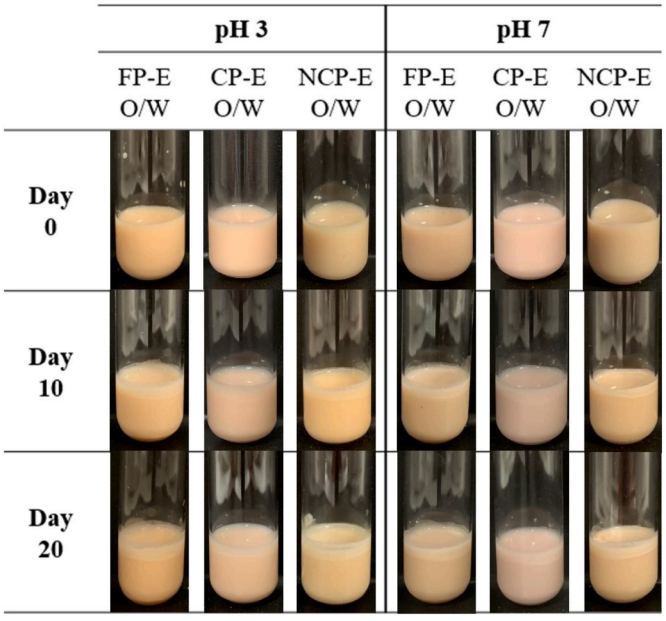

Fig. 6. Visual appearance during 20 days of storage at 4 °C of oil-in-water (O/W) emulsions of corn oil (2% w/w) stabilized with persimmon pectin extracts in aqueous solution (1% w/w) differing in polyphenol-pectin interactions, being free phenolics-extract (FP-E), covalent phenolics-extract (CP-E) and non-covalent phenolics-extract (NCP-E), at pH 3 and 7.

3.4.2. Colloidal stability of the O/W emulsions throughout storage

The homogeneous visual appearance of O/W emulsions after preparation changed to heterogenous with the storage time, since a creamed layer appeared at the top part of the tub (Fig. 6). Regardless of the pH, this creamed layer appeared earlier in those O/W emulsions formulated using FP-E or NCP-E, than in the case of CP-E-stabilized O/W emulsions. Similarly, phase contrast microscopy images of the O/W emulsions stabilized with FP-E and NCP-E showed particle aggregation after 10 and 20 days of storage at pH 3 and 7, respectively (Figs. 8 and 9). In contrast, O/W emulsions stabilized with CP-E had particles homogeneously dispersed without aggregation along the storage time, regardless of the pH. This suggests that CP-E rendered O/W emulsions with higher colloidal stability than FP-E or NCP-E. Nevertheless, the average particle size and ζ-potential of the O/W emulsions during storage time did not present variations, regardless of the persimmon pectin extract and the pH of its solution (Supplementary Material Figs. S1 and S2). Thus, the creaming phenomena observed visually and the aggregation shown in the microscopy images could be attributed to depletion flocculation

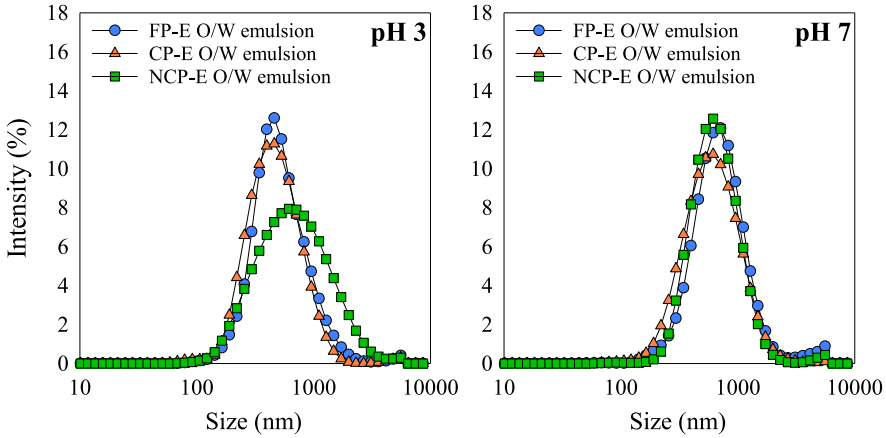

Fig. 7. Particle size distribution in intensity (%) of oil-in-water (O/W) emulsions of corn oil (2% w/w) stabilized with persimmon pectin extracts in aqueous solution (1% w/w) differing in polyphenol-pectin interactions, being free phenolics-extract (FP-E), covalent phenolics-extract (CP-E) and non-covalent phenolics-extract (NCP-E), after preparation, measured at both pH 3 and 7.

Table 4
Average particle size (nm), PDI and ζ-potential (mV) after preparation of oil-in-water (O/W) emulsions of corn oil (2% w/w) stabilized with persimmon pectin extracts in aqueous solution (1% w/w) differing in polyphenol-pectin interactions, being free phenolics-extract (FP-E), covalent phenolics-extract (CP-E) and non-covalent phenolics-extract (NCP-E), measured at both pH 3 and 7. A,B letters mean significant differences between different formulations for the same pH. a,b letters indicate significant differences between different pH for the same formulation.

	Particle size (nm)		PDI		ζ-potential (mV)	
	pH 3	pH 7	pH 3	pH 7	pH 3	pH 7
FP-E O/W emulsion	532.40 ± 28.57^{Aa}	656.13 ± 46.72^{Aa}	0.36 ± 0.14^{Aa}	0.31 ± 0.11^{Aa}	-21.06 ± 0.27^{Aa}	-57.98 ± 11.67^{Ab}
CP-E O/W emulsion	402.63 ± 41.27^{Aa}	505.80 ± 67.06^{Aa}	0.23 ± 0.03^{Aa}	0.25 ± 0.003^{Aa}	-16.21 ± 0.79^{Ba}	-49.48 ± 4.80^{Ab}
NCP-E O/W emulsion	549.38 ± 77.75^{Aa}	569.05 ± 5.35^{Aa}	0.31 ± 0.08^{Aa}	0.23 ± 0.004^{Aa}	-21.21 ± 0.22^{Aa}	-59.03 ± 4.54^{Ab}

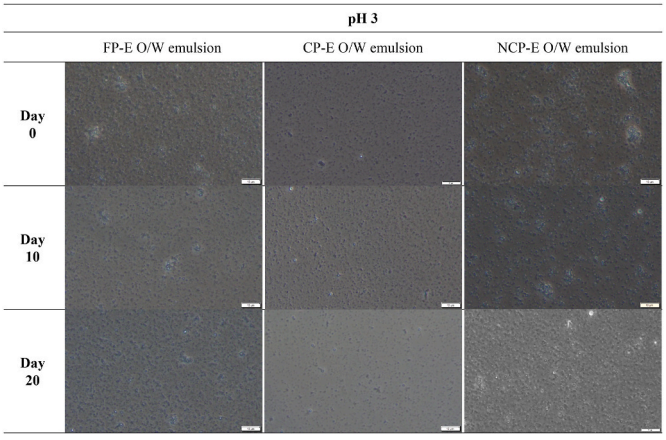

Fig. 8. Phase contrast microscopy images of oil-in-water (O/W) emulsions of corn oil (2% w/w) stabilized with persimmon pectin extracts in aqueous solution (1% w/w) differing in polyphenol-pectin interactions, being free phenolics-extract (FP-E), covalent phenolics-extract (CP-E) and non-covalent phenolics-extract (NCP-E), measured at pH 3. Scale bar: 10 μm.

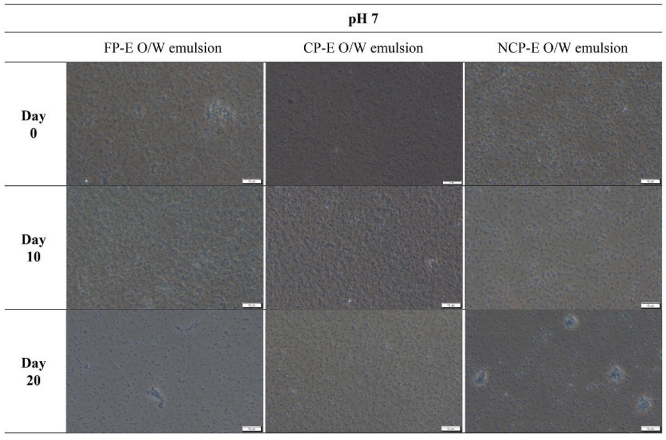

Fig. 9. Phase contrast microscopy images of oil-in-water (O/W) emulsions of corn oil (2% w/w) stabilized with persimmon pectin extracts in aqueous solution (1 % w/w) differing in polyphenol-pectin interactions, being free phenolics-extract (FP-E), covalent phenolics-extract (CP-E) and non-covalent phenolics-extract (NCP-E), measured at pH 7. Scale bar: 10 μm.

rather than coalescence of the oil droplets (Dickinson, 2003).

4. Conclusions

The present study provides useful information about the influence of persimmon pectin structural characteristics and its interaction with polyphenols on their molecular structure and conformation in solution as well as interfacial and emulsification properties at pH 3 or 7. In this regard, the electrical charge of pectin in aqueous solutions was shown to be dependent on the pH rather than pectin structure characteristics or interactions with polyphenols. Regarding its molecular structure and conformation in solution, it might be influenced by pectin-polyphenol interactions. The organization of pectin at interfaces was evidenced to be mainly influenced by the pH. Moreover, it was demonstrated that persimmon pectin presents surface-active properties that can vary depending on its structural characteristics, interactions with

polyphenols and pH. O/W emulsions with submicron particle size could be formed using pectin as emulsifier, yet their colloidal stability was shown to be influenced by its interaction with polyphenols. Hence, this work provides novel insights into the re-valorization of persimmon pectin from the food chain as emulsifier and the possibility of modulating their molecular structure in solution and emulsification properties depending on their structural characteristics and interaction with polyphenols.

CRediT authorship contribution statement

Anna Molet-Rodríguez: Writing – original draft, Visualization, Methodology, Investigation, Formal analysis. **Daniel A. Méndez:** Methodology, Investigation, Formal analysis. **Amparo López-Rubio:** Writing – review & editing, Project administration, Methodology, Funding acquisition, Formal analysis, Conceptualization. **María José Fabra:** Writing – review & editing, Methodology, Formal analysis, Conceptualization. **Marta Martínez-Sanz:** Writing – review & editing, Methodology, Investigation, Formal analysis, Conceptualization. **Laura Salvia-Trujillo:** Writing – review & editing, Visualization, Supervision, Project administration, Methodology, Funding acquisition, Conceptualization. **Olga Martín-Belloso:** Writing – review & editing, Visualization, Supervision, Project administration, Funding acquisition, Conceptualization.

Declaration of competing interest

The authors declare that they have no known competing financial interests or personal relationships that could have appeared to influence the work reported in this paper.

Data availability

Data will be made available on request.

Acknowledgements

This study was funded by the Ministry of Economy, Industry and Competitiveness (MINECO/FEDER, UE) throughout projects RTI2018-094268-B-C2 and PID2022-137838OB-I00. Project INNEST/2021/27 was granted by Agencia Valenciana de Innovación (AVI) and co-financed by the European Union through the Operative Programme of FEDER from Comunitat Valenciana 2014–2020. The Accreditation of IATA-CSIC as Center of Excellence Severo Ochoa CEX2021-001189-S funded by MCIU/AEI/10.13039/501100011033 is also fully acknowledged.

Appendix A. Supplementary data

Supplementary data to this article can be found online at https://doi.org/10.1016/j.foodhyd.2024.110553.

References

Alba, K., & Kontogiorgos, V. (2017). Pectin at the oil-water interface: Relationship of molecular composition and structure to functionality. *Food Hydrocolloids, 68*, 211–218. https://doi.org/10.1016/j.foodhyd.2016.07.026

Assifaoui, A., Hayrapetyan, G., Gallery, C., & Agoda-Tandjawa, G. (2024). Exploring techno-functional properties, synergies, and challenges of pectins: A review. *Carbohydrate Polymer Technologies and Applications, 7*. https://doi.org/10.1016/j.carpta.2024.100496. Article 100496.

Beaucage, G. (1995). Approximations leading to a unified exponential/power-law approach to small-angle scattering. *Journal of Applied Crystallography, 28*(6), 717–728. https://doi.org/10.1107/s0021889895005292

Beaucage, G. (1996). Small-angle scattering from polymeric mass fractals of arbitrary mass-fractal dimension. *Journal of Applied Crystallography, 29*(2), 134–146. https://doi.org/10.1107/S0021889895011605

Bindereif, B., Karbstein, H. P., Zahn, K., & van der Schaaf, U. S. (2022). Effect of conformation of sugar beet pectin on the interfacial and emulsifying properties. *Foods, 11*(2). https://doi.org/10.3390/foods11020214

Caffall, K. H., & Mohnen, D. (2009). The structure, function, and biosynthesis of plant cell wall pectic polysaccharides. *Carbohydrate Research, 344*(14), 1879–1900. https://doi.org/10.1016/j.carres.2009.05.021

Chandel, V., Biswas, D., Roy, S., Vaidya, D., Verma, A., & Gupta, A. (2022). Current advancements in pectin: Extraction, properties and multifunctional applications. *Foods, 11*(17), 1–30. https://doi.org/10.3390/foods11172683

Christiaens, S., Uwibambe, D., Uyttebroek, M., Van Droogenbroeck, B., Van Loey, A. M., & Hendrickx, M. E. (2015). Pectin characterisation in vegetable waste streams: A starting point for waste valorisation in the food industry. *Lwt, 61*(2), 275–282. https://doi.org/10.1016/j.lwt.2014.12.054

Cui, J., Ren, W., Zhao, C., Gao, W., Tian, G., Bao, Y., et al. (2020). The structure–property relationships of acid- and alkali-extracted grapefruit peel pectins. *Carbohydrate Polymers, 229*. https://doi.org/10.1016/j.carbpol.2019.115524. Article 115524.

Di Mattia, C. D., Sacchetti, G., Mastrocola, D., Sarker, D. K., & Pittia, P. (2010). Surface properties of phenolic compounds and their influence on the dispersion degree and oxidative stability of olive oil O/W emulsions. *Food Hydrocolloids, 24*(6–7), 652–658. https://doi.org/10.1016/j.foodhyd.2010.03.007

Dickinson, E. (2003). Hydrocolloids at interfaces and the influence on the properties of dispersed systems. *Food Hydrocolloids, 17*(1), 25–39. https://doi.org/10.1016/S0268-005X(01)00120-5

Dickinson, E. (2009). Hydrocolloids as emulsifiers and emulsion stabilizers. *Food Hydrocolloids, 23*(6), 1473–1482. https://doi.org/10.1016/j.foodhyd.2008.08.005

Dranca, F., Vargas, M., & Oroiana, M. (2020). Physicochemical properties of pectin from Malus domestica 'Fălticeni' apple pomace as affected by non-conventional extraction techniques. *Food Hydrocolloids, 100*. https://doi.org/10.1016/j.foodhyd.2019.105383. Article 105383.

Einhorn-Stoll, U., Kastner, H., Hecht, T., Zimathies, A., & Drusch, S. (2015). Modification and physico-chemical properties of citrus pectin - influence of enzymatic and acidic demethoxylation. *Food Hydrocolloids, 51*, 338–345. https://doi.org/10.1016/j.foodhyd.2015.05.031

Friedman, M., & Jürgens, H. S. (2000). Effect of pH on the stability of plant phenolic compounds. *Journal of Agricultural and Food Chemistry, 48*(6), 2101–2110. https://doi.org/10.1021/jf990489j

Funami, T., Zhang, G., Hiroe, M., Noda, S., Nakauma, M., Asai, I., et al. (2007). Effects of the proteinaceous moiety on the emulsifying properties of sugar beet pectin. *Food Hydrocolloids, 21*(8), 1319–1329. https://doi.org/10.1016/j.foodhyd.2006.10.009

Gleeson, J. P., Ryan, S. M., & Brayden, D. J. (2016). Oral delivery strategies for nutraceuticals: Delivery vehicles and absorption enhancers. *Trends in Food Science and Technology, 53*, 90–101. https://doi.org/10.1016/j.tifs.2016.05.007

Humerez-Flores, J. N., Verkempinck, S. H. E., Van Loey, A. M., Moldenaers, P., & Hendrickx, M. E. (2022). Targeted modifications of citrus pectin to improve interfacial properties and the impact on emulsion stability. *Food Hydrocolloids, 132*, Article 107841. https://doi.org/10.1016/j.foodhyd.2022.107841

Iijima, M., Nakamura, K., Hatakeyama, T., & Hatakeyama, H. (2000). Phase transition of pectin with sorbed water. *Carbohydrate Polymers, 41*(1), 101–106. https://doi.org/10.1016/S0144-8617(99)00116-2

Ilavsky, J., & Jemian, P. R. (2009). Irena: Tool suite for modeling and analysis of small-angle scattering. *Journal of Applied Crystallography, 42*(2), 347–353. https://doi.org/10.1107/S0021889809002222

Jakobek, L., & Matić, P. (2019). Non-covalent dietary fiber - polyphenol interactions and their influence on polyphenol bioaccessibility. *Trends in Food Science and Technology, 83*, 235–247. https://doi.org/10.1016/j.tifs.2018.11.024

Jia, Y., Du, J., Li, K., & Li, C. (2022a). Emulsification mechanism of persimmon pectin with promising emulsification capability and stability. *Food Hydrocolloids, 131*, Article 107727. https://doi.org/10.1016/j.foodhyd.2022.107727

Jia, Y., Khalifa, I., Dang, M., Zhang, Y., Zhu, L., Zhao, M., et al. (2022b). Confirmation and understanding the potential emulsifying characterization of persimmon pectin: From structural to diverse rheological aspects. *Food Hydrocolloids, 131*, Article 107738. https://doi.org/10.1016/j.foodhyd.2022.107738

Jiang, Y., Xu, Y., Li, F., Li, D., & Huang, Q. (2020). Pectin extracted from persimmon peel: A physicochemical characterization and emulsifying properties evaluation. *Food Hydrocolloids, 101*, Article 105561. https://doi.org/10.1016/j.foodhyd.2019.105561

Kieffer, J., & Ashiotis, G. (2014). PyFAI: A Python library for high performance azimuthal integration on GPU. *Powder Diffraction, 28*(SUPPL.2), 3.

Kralova, I., & Sjöblom, J. (2009). Surfactants used in food industry: A review. *Journal of Dispersion Science and Technology, 30*(9), 1363–1383. https://doi.org/10.1080/01932690902735561

Le Bourvellec, C., Bouchet, B., & Renard, C. M. G. C. (2005). Non-covalent interaction between procyanidins and apple cell wall material. Part III: Study on model polysaccharides. *Biochimica et Biophysica Acta (BBA) - General Subjects, 1725*(1), 10–18. https://doi.org/10.1016/j.bbagen.2005.06.004

Leroux, J., Langendorff, V., Schick, G., Vaishnav, V., & Mazoyer, J. (2003). Emulsion stabilizing properties of pectin. *Food Hydrocolloids, 17*(4), 455–462. https://doi.org/10.1016/S0268-005X(03)00027-4

Luo, J., Wang, Z. W., Wang, F., Zhang, H., Lu, J., Guo, H. Y., et al. (2014). Cryo-SEM images of native milk fat globule indicate small casein micelles are constituents of the membrane. *RSC Advances, 4*(90), 48963–48966. https://doi.org/10.1039/c4ra06171c

McClements, D. J. (2015). *Food emulsions: Principles, practices, and techniques* (3rd ed.). Boca Raton, FL: CRC Press.

Mendez, D. A., Fabra, M. J., Martínez-Abad, A., Martínez-Sanz, M., Gorria, M., & López-Rubio, A. (2021). Understanding the different emulsification mechanisms of pectin:

Comparison between watermelon rind and two commercial pectin sources. *Food Hydrocolloids, 120*, Article 106957. https://doi.org/10.1016/j.foodhyd.2021.106957

Méndez, D. A., Fabra, M. J., Odriozola-Serrano, I., Martín-Belloso, O., Salvia-Trujillo, L., López-Rubio, A., et al. (2022). Influence of the extraction conditions on the carbohydrate and phenolic composition of functional pectin from persimmon waste streams. *Food Hydrocolloids, 123*, Article 107066. https://doi.org/10.1016/j.foodhyd.2021.107066

Méndez, D. A., Martínez-Abad, A., Martínez-Sanz, M., López-Rubio, A., & Fabra, M. J. (2023). Tailoring structural, rheological and gelling properties of watermelon rind pectin by enzymatic treatments. *Food Hydrocolloids, 135*, Article 108119. https://doi.org/10.1016/j.foodhyd.2022.108119

Molet-Rodríguez, A., Salvia-Trujillo, L., & Martín-Belloso, O. (2018). Beverage emulsions: Key aspects of their formulation and physicochemical stability. *Beverages, 4*(3), 70. https://doi.org/10.3390/beverages4030070

Morris, G. A., Foster, T. J., & Harding, S. E. (2000). The effect of the degree of esterification on the hydrodynamic properties of citrus pectin. *Food Hydrocolloids, 14*(3), 227–235. https://doi.org/10.1016/S0268-005X(00)00007-2

Ngouémazong, E. D., Christiaens, S., Shpigelman, A., Van Loey, A., & Hendrickx, M. (2015). The emulsifying and emulsion-stabilizing properties of pectin: A review. *Comprehensive Reviews in Food Science and Food Safety, 14*(6), 705–718. https://doi.org/10.1111/1541-4337.12160

Niu, H., Chen, X., Luo, T., Chen, H., & Fu, X. (2022). Relationships between the behavior of three different sources of pectin at the oil-water interface and the stability of the emulsion. *Food Hydrocolloids, 128*, Article 107566. https://doi.org/10.1016/j.foodhyd.2022.107566

Osorio, C., Carriazo, J. G., & Barbosa, H. (2011). Thermal and structural study of guava (Psidium Guajava L) powders obtained by two dehydration methods. *Quimica Nova, 34*(4), 636–640. https://doi.org/10.1590/S0100-40422011000400016

Pereira, L. M., Carmello-Guerreiro, S. M., & Hubinger, M. D. (2009). Microscopic features, mechanical and thermal properties of osmotically dehydrated guavas. *Lwt, 42*(1), 378–384. https://doi.org/10.1016/j.lwt.2008.06.002

Santiago, J. S., Salvia-Trujillo, L., Palomo, A., Niroula, A., Xu, F., Van Loey, A. M., et al. (2018). Process-induced water-soluble biopolymers from broccoli and tomato purées: Their molecular structure in relation to their emulsion stabilizing capacity. *Food Hydrocolloids, 81*, 312–327. https://doi.org/10.1016/j.foodhyd.2018.03.005

Schmidt, U. S., Koch, L., Rentschler, C., Kurz, T., Endreß, H. U., & Schuchmann, H. P. (2015). Effect of molecular weight reduction, acetylation and esterification on the emulsification properties of citrus pectin. *Food Biophysics, 10*(2), 217–227. https://doi.org/10.1007/s11483-014-9380-1

Schmidt, U. S., Schütz, L., & Schuchmann, H. P. (2017). Interfacial and emulsifying properties of citrus pectin: Interaction of pH, ionic strength and degree of esterification. *Food Hydrocolloids, 62*, 288–298. https://doi.org/10.1016/j.foodhyd.2016.08.016

Shuai, X., Chen, J., Liu, Q., Dong, H., Dai, T., Li, Z., et al. (2022). The effects of pectin structure on emulsifying, rheological, and in vitro digestion properties of emulsion. *Foods, 11*(21), 3444. https://doi.org/10.3390/foods11213444

Siew, C. K., Williams, P. A., Cui, S. W., & Wang, Q. (2008). Characterization of the surface-active components of sugar beet pectin and the hydrodynamic thickness of the adsorbed pectin layer. *Journal of Agricultural and Food Chemistry, 56*(17), 8111–8120. https://doi.org/10.1021/jf801588a

Velderrain-Rodríguez, G. R., Salvia-Trujillo, L., González-Aguilar, G. A., & Martín-Belloso, O. (2021). Interfacial activity of phenolic-rich extracts from avocado fruit waste: Influence on the colloidal and oxidative stability of emulsions and nanoemulsions. *Innovative Food Science and Emerging Technologies, 69*. https://doi.org/10.1016/j.ifset.2021.102665. Article 102665.

Verkempinck, S. H. E., Kyomugasho, C., Salvia-Trujillo, L., Denis, S., Bourgeois, M., Van Loey, A. M., et al. (2018). Emulsion stabilizing properties of citrus pectin and its interactions with conventional emulsifiers in oil-in-water emulsions. *Food Hydrocolloids, 85*, 144–157. https://doi.org/10.1016/j.foodhyd.2018.07.014

Wang, X., Chen, Q., & Lü, X. (2014). Pectin extracted from apple pomace and citrus peel by subcritical water. *Food Hydrocolloids, 38*, 129–137. https://doi.org/10.1016/j.foodhyd.2013.12.003